Monomer–Dimer Solution Equilibria of 2,4,6-Trialkylnitrosobenzenes and 2,4,6-Trialkylnitrosobenzene/Nitrosobenzene Mixtures. A Study Using One- and Two-dimensional NMR Techniques

Keith G. Orrell,* David Stephenson, and James H. Verlaque
Department of Chemistry, The University, Exeter EX4 4QD

2,4,6-Trimethylnitrosobenzene in $CDCl_3$ exists as a mixture of monomer and *Z*- and *E*-azodioxy dimers. The dissociation kinetics of both dimers were measured by one-dimensional time-dependent NMR spectroscopy on non-equilibrium solutions, and by two-dimensional exchange spectroscopy (2D-EXSY) on equilibrium solutions. 2,4,6-Tri-t-butylnitrosobenzene is entirely monomeric in $CDCl_3$ but forms mixed azodioxy dimers in the presence of nitrosobenzene. The dissociation kinetics of the mixed *E*-dimer were followed by NMR techniques. The activation energy parameters for these dissociation equilibria were compared with previous data on related nitrosobenzene and dimethylnitrosobenzene systems.

C-Nitroso compounds have been extensively investigated over a number of decades,[1–5] and much is now firmly established concerning their solid-state and solution structures. In essence, the compounds can exist as intense blue or green monomers or as colourless dimers, with the dimeric structures being most usual in the solid state. In organic solvents, monomer–dimer equilibria are established with the predominant solution species depending sensitively on their electronic and steric natures. In the case of aromatic *C*-nitroso compounds, the nature of any ring substituent(s) controls the population distribution of the three possible solution species, namely monomer (**1**), *Z*-azodioxy dimer (**2**), or *E*-azodioxy dimer (**3**).

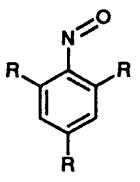

(1)

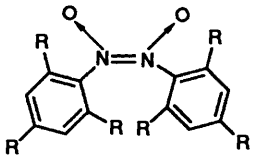

(2)

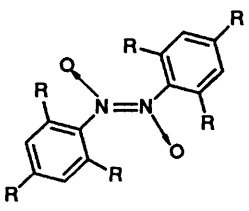

(3)

In earlier studies of aromatic *C*-nitroso compounds, X-ray crystallography,[6–8] IR spectroscopy,[9–11] and UV–visible spectrophotometry[12–14] have been employed in establishing their solid-state structures and solution equilibria. Whilst these techniques have provided much valuable information, it has recently been shown by us[15,16] that modern solution NMR techniques can provide further insight into these systems, by providing an unequivocal distinction between *Z*- and *E*-dimeric species and affording accurate kinetic data on the dissociation of these species to monomers. These earlier studies centred on nitrosobenzene (NB)[15] and dimethylnitrosobenzenes (DMNB)[16] and led to the first identification of the *E*-azodioxy dimer of nitrosobenzene, *E*-$(NB)_2$, and the *Z*-dimer of 2,6-dimethylnitrosobenzene, *Z*-$(2,6\text{-DMNB})_2$. In related studies on mixed systems (*e.g.* 2,6-DMNB + NB), both *Z*- and *E*-mixed dimers were identified.[16] Earlier literature reports of mixed aromatic nitroso dimers have arisen from solid–liquid equilibrium studies[17] and photochemical experiments.[18] A recent report of mixed aliphatic–aromatic nitroso dimers involved ^1H NMR spectroscopy to establish association constants.[19] However, in none of these studies were the isomeric forms of the dimers established.

We now report on 2,4,6-trimethylnitrosobenzene (2,4,6-TMNB)[20] in $CDCl_3$ solution and demonstrate how a combination of one-dimensional time-dependent NMR (1D-TD) and two-dimensional NMR exchange studies (2D-EXSY) can provide definitive structural and kinetic data on all solution species present over a wide temperature range.

We have also applied similar NMR techniques to 2,4,6-tri-t-butylnitrosobenzene (2,4,6-TBNB)[21] in $CDCl_3$. This compound is an important spin-trapping agent[22] with both atoms of its nitroso function serving as trapping sites.[23] It is also particularly stable in solution, even during photolysis, and has no tendency to dimerise either in solution or in the solid state. In the light of our earlier studies[16] we wished to test whether there was any tendency for 2,4,6-TBNB to dimerise in the presence of other sterically less hindered nitrosobenzenes, as such information would be of relevance to its radical scavenging properties.

Experimental

Materials.—Nitrosobenzene (NB) and 2,4,6-tri-t-butylnitrosobenzene (2,4,6-TBNB) were purchased from Aldrich. 2,4,6-Trimethylnitrosobenzene (2,4,6-TMNB) was prepared from its nitro derivative by reduction with zinc and ammonium chloride to the hydroxylamine compound followed by oxidation to the nitroso derivative.[24] The following procedure was found to minimise side reactions. A solution/suspension of 2,4,6-TMNB (4 g, 0.027 mol), ammonium chloride (2 g, 0.037 mol) and zinc powder (4 g) in acetone (20 cm^3) was cooled to 0 °C, and water added dropwise until reaction occurred as indicated by a sharp temperature rise. Water was added more cautiously as the reaction slowed and the temperature was not allowed to rise above 10 °C. When the reaction ceased, the mixture was poured into ice-cold water (200 cm^3) and then

Table 1. Proton chemical shifts of 2,4,6-TMNB in $CDCl_3$[a] at 243 K.

	δ[b]		
Assignment	2,4,6-TMNB	*E*-(2,4,6-TMNB)$_2$	*Z*-(2,4,6-TMNB)$_2$
Aromatic	7.01	7.01	6.77
2,6-Me	2.63	2.41	2.12
4-Me	2.35	2.32	2.22

[a] 0.1 mol dm^{-3} solution. [b] Relative to internal $SiMe_4$.

Table 2. Population studies of 2,4,6-TMNB *E*-dimer–monomer equilibrium.

	% Population[a]		
T/K	Monomer	*E*-Dimer	K°[b]
333	85.0	15.0	4.82
323	75.7	24.3	2.36
313	63.3	36.7	1.09
303	51.8	48.2	0.56
293	39.1	60.9	0.25

[a] Values ±0.05. [b] Equilibrium constant values refer to *E*-(2,4,6-TMNB) $\rightleftharpoons$ 2 (2,4,6-TMNB) $K^{\circ} = [M]^2/[D]c^{\circ}$ where $c^{\circ} = 1$ mol dm^{-3}.

filtered. Iron(III) chloride solution (3 g $FeCl_3$ in 10 cm^3 water) was added to the filtrate. After *ca.* 5 min a precipitate of 2,4,6-TMNB formed which was filtered off and recrystallised from chloroform.

NMR Studies.—Proton spectra were recorded at a frequency of 250.1 MHz on a Bruker AM250 spectrometer equipped with an ASPECT 3000 computer. Variable temperature measurements were made with a standard B-VT100 unit, the temperature reliability of which was checked periodically against a Comark digital thermometer. The quoted spectral temperatures are estimated to be accurate to at least ±1 °C.

One-dimensional time-dependent (1D-TD) spectra were recorded every 30 or 60 s for non-equilibrium samples. For each temperature, 8–16 spectra were taken in most cases. Each spectrum was the result of a single pulse, a time-domain of 8K words and an acquisition time of 1.6 s. Free-induction decays of each spectrum were stored on disk and data processing (Fourier transformation and signal integrations) performed later.

Two-dimensional ^{1}H EXSY spectra (2D-EXSY) were obtained in the pure absorption mode using the Bruker automation program NOESYPH, which uses the pulse sequence D1-90°-D0-90°-D9-90°-FID. In all cases a spectral width of 150 Hz, an F2 dimension of 512 W, and an F1 dimension of 128 W, zero filled to 512 W, were employed. It has been shown previously[16] that values of the initial relaxation delay, D1, in the range 2–6 s have a negligible effect on the calculated exchange rates. A value of 3 s was, therefore, chosen for D1, this being a compromise between signal/noise ratio of the resulting spectra and the speed with which these spectra were acquired. Optimal values of the mixing times D9 ($=\tau_m$) were in the range 1–1.5 s (see below). Spectra were processed using a Gaussian window function (Bruker software parameters, GB = 0.0, LB = 0.2 Hz). Signal volume intensities were obtained from unsymmetrized spectra and processed to give exchange rate constants using the D2DNMR program as described previously.[25] Symmetrization of the 2D spectral map was not performed in order to avoid confusion with spectral artifacts such as t_1 noise, and because the computational procedure takes into account any asymmetry in the 2D data.

Results

2,4,6-Trimethylnitrosobenzene (2,4,6-TMNB).—^{1}H NMR spectra of a 0.1 mol dm^{-3} * solution of 2,4,6-TMNB in $CDCl_3$ were recorded in the temperature range 223 to 333 K. At ambient temperatures (283–333 K) aromatic and methyl signals due to monomeric 2,4,6-TMNB and a single dimeric species of 2,4,6-TMNB were detected. On cooling the solution to 223 K, the monomer signals diminished in intensity and additional signals, attributed to the other dimer, appeared. By comparison with the solution properties of 2,6-dimethylnitrosobenzene (2,6-DMNB),[16] the more populous dimer was attributed with confidence to *E*-(2,4,6-TMNB)$_2$ (3; R = Me). The methyl ^{1}H chemical shifts of all three solution species, measured at 243 K, are collected in Table 1. The corresponding values for (2,6-DMNB)$_2$ at 233 K namely, δ 2.48 (*E*) and δ 2.18 (*Z*),[16] strongly support the assignments shown in Table 1.

Relative populations of 2,4,6-TMNB and *E*-(2,4,6-TMNB)$_2$ were measured in the temperature range 293 to 333 K, in which range the concentration of *Z*-(2,4,6-TMNB) was negligible. The percentage populations (Table 2) were based on the relative intensities of the 2,6-methyl signals.

Thermodynamic data for the equilibrium, Scheme 1, were

E-(2,4,6-TMNB)$_2$ $\rightleftharpoons$ 2 (2,4,6-TMNB)

Scheme 1.

derived from the plot of ln K° against T^{-1}, the data obtained being as follows ΔH° 59.7 ± 1.3 kJ mol^{-1}, ΔS° 192 ± 4 J K^{-1} mol^{-1}, ΔG° (298.15 K) 2.5 ± 0.1 kJ mol^{-1}.

These values should be compared with the corresponding values for the 2,6-DMNB system, namely ΔH° 94.2 kJ mol^{-1}, ΔS° 278 J K^{-1} mol^{-1}, and ΔG° (298.15 K) 11.4 kJ mol^{-1}. The positive ΔH° values indicate that the *E*-dimer, *E*-(2,4,6-TMNB)$_2$ is thermodynamically favoured over the 2,4,6-TMNB monomer, but this preference is not as strong as in the 2,6-DMNB system. The large, positive ΔS° value is typical of dissociation equilibria.

A preliminary examination of the ^{1}H NMR spectra of 2,4,6-TMNB in $CDCl_3$ in the range 223–333 K showed that the *Z*-dimer was present in detectable amounts between 223 and 263 K. Above this temperature, it underwent fast exchange with the monomer and was not detectable as a separate solution species. The changes in the NMR spectra above 263 K were due to the relatively slow dissociation of *E*-dimer to the monomer. In order to obtain kinetic data of optimum accuracy from NMR experiments in the full temperature range 223–333 K four sets of experiments were planned, as described below.

Time-dependent NMR studies, 223–243 K. In this temperature range the kinetics of the reversible *Z*-dimer–monomer exchange of 2,4,6-TMNB were measured on a 0.1 mol dm^{-3} $CDCl_3$ solution which was quickly cooled from *ca.* 60 °C to low temperature thus effectively 'freezing' the *E*-dimer concentration at a constant value by virtue of its very slow dissociation rate on the NMR time-scale. The increase in the concentration of *Z*-(2,4,6-TMNB)$_2$ as equilibrium was established with monomeric 2,4,6-TMNB was monitored by the change in relative intensities of the 2,6-methyl signals of the monomer and *Z*-dimer.

For the reversible exchanging system, Scheme 2, which

$$Z\text{-D} \underset{k_{-1}}{\overset{k_1}{\rightleftharpoons}} 2\text{M}$$

Scheme 2.

* Molarity based on 100% 2,4,6-TMNB monomer.

Table 3. Rate data for *Z*-(2,4,6-TMNB)$_2$ ⟶ 2 (2,4,6-TMNB) exchange.

NMR method	*T*/K	10^3K/*T*	*k*/s^{-1}	ln(*k*/*T*)
1D-TD	223	4.484	3.76×10^{-5}	−15.60
	233	4.292	3.08×10^{-4}	−13.52
	243	4.115	2.61×10^{-3}	−11.46
2D-EXSY	253	3.953	1.36×10^{-2}	−9.83
	263	3.802	4.46×10^{-2}	−8.68

involves a combination of first- and second-order kinetics, we can, therefore, write equation (1). At equilibrium d[D]/dt = 0,

$$\frac{d[D]}{dt} = k_{-1}[M]^2 - k_1[D] \quad (1)$$

and hence $k_{-1} = k_1[D]_e/[M]_e^2$, where the e subscripts refer to equilibrium conditions. The total solution concentration, c, based on 2,4,6-TMNB monomer moieties, is, therefore, [M] + 2[D]. The concentrations of either species cannot be assumed to be negligible at any time. We have shown previously[16] that such a kinetic system obeys the rate law, equation (2),

$$\ln\left(\frac{x[D]_t + a}{y[D]_t + b}\right) = -q_D k_1 t \quad (2)$$

where

$$a = [D]_e(-c^2 + 4[D]_o[D]_e) = -[D]_e x$$
$$b = c^2([D]_o - [D]_e)$$
$$x = c^2 - 4[D]_o[D]_e$$
$$y = 4([D]_e^2 - [D]_o[D]_e) = -4[D]_e b/c^2$$
$$q_D = (c + 2[D]_e)/(c - 2[D]_e)$$

and $[D]_o$, $[D]_t$, $[D]_e$ refer to *Z*-D concentrations at times $t = 0$, $t = t$, and $t = \infty$(equilibrium) respectively. First-order rate constants, k_1, were computed from the slope of the graph of the logarithmic function of equation (2) *vs.* time. Values for the three temperatures studied are collected in Table 3.

2D-EXSY *NMR studies*, 253–263 K. In recent years two-dimensional NMR exchange spectroscopy (2D-EXSY) has established itself as a powerful kinetic tool, particularly for measuring multi-site exchange processes.[26] It represents the 2D analogue of selective magnetization transfer experiments,[27] and can be applied to molecular rate processes which are sufficiently slow so that NMR band broadening effects are minimal. The technique is based on the NOESY pulse sequence, D1-90°-D0-90°-D9-90°-FID,[28] where D9 is the mixing time (τ_m) during which spin transfer occurs as a result of the exchange process, causing cross-peak signals to appear between exchanging diagonal signals in the 2D spectral map. The technique can be used for quantitative kinetic studies,[25–31] providing that signals due to cross-relaxation effects and multiple quantum coherences (MQCs) are either negligible or separated out. In the present studies MQCs did not occur since the methyl signals, used for monitoring the exchange processes, did not exhibit any scalar couplings with other protons, and intermolecular cross-relaxation effects of methyl groups in monomer and dimer species were likely to be negligibly weak.

In this temperature range the exchange rates associated with Scheme 3 come within the range of detection of 2D-EXSY NMR

$$Z\text{-D} \rightleftharpoons 2\text{M}$$

Scheme 3.

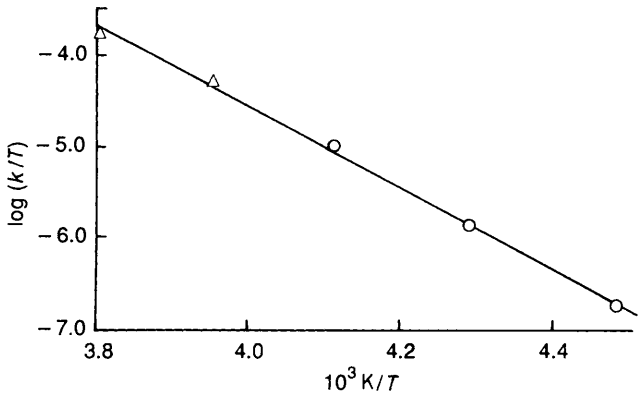

Figure 1. Eyring plot of rate data for the *Z*-(2,4,6-TMNB)$_2$ ⟶ 2(2,4,6-TMNB) dissociation, using time-dependent 1D NMR data (○) and 2D-EXSY NMR data (△).

experiments. Proton 2D-EXSY spectra were, therefore, recorded at temperatures 253 K and 263 K using an optimal mixing time, τ_m, of 1 s. In the methyl region, well-defined diagonal and cross-peaks were obtained for both the 2,6- and 4-methyl signals of 2,4,6-TMNB and *Z*-(2,4,6-TMNB)$_2$, with the 2,6-methyl signals being more conveniently situated for intensity measurements. Volume integrals of these signals were, therefore, obtained and after normalisation, used in the computer program D2DNMR[25] to generate the kinetic matrix for the system from which the rate constants for the dissociation *Z*-D ⟶ 2M were calculated. The values, given in Table 3, were then combined with the 1D-time-dependent NMR values, and standard Eyring rate theory applied to yield the activation parameters for the dissociation process (Table 4). The Eyring plot (Figure 1) shows the good correlation of the 1D- and 2D-NMR-derived rate data.

Time-dependent NMR studies, 273–283 K. In this temperature range the *Z*-dimer and monomer species were at equilibrium and the reversible kinetics of the *E*-dimer–monomer exchange were followed by measuring the change in the 2,6-methyl signal of the monomer species as a function of time according to the kinetic treatment shown in Scheme 4.

$$E\text{-D} \underset{k_{-1}}{\overset{k_1}{\rightleftharpoons}} 2\text{M} \overset{\text{fast}}{\rightleftharpoons} Z\text{-D}$$

Scheme 4.

Total concentration in terms of monomer moieties, c, is given by equation (3).

$$c = 2[E\text{-D}] + 2[Z\text{-D}] + [M] \quad (3)$$

Since the *Z*-dimer and monomer species are at equilibrium $K_e = [Z\text{-D}]/[M]^2$ and we can write equation (4).

$$\frac{d[Z\text{-D}]}{dt} = 2K_e[M]\frac{d[M]}{dt} \quad (4)$$

From Scheme 4 we can write equations (5) and (6).

$$\frac{d[M]}{dt} = 2k_1[E\text{-D}] - 2k_{-1}[M]^2 - 4K_e[M]\frac{d[M]}{dt} \quad (5)$$

$$\frac{d[E\text{-D}]}{dt} = k_{-1}[M]^2 - k_1[E\text{-D}] \quad (6)$$

At equilibrium $\frac{d[E\text{-D}]}{dt} = 0$.

Table 4. Activation parameters for the monomer–dimer equilibria of 2,4,6-trialkylnitrosobenzenes in $CDCl_3$.

System	NMR technique	Temp. range/K	$\Delta H^{\ddagger}$/kJ mol^{-1}	$\Delta S^{\ddagger}$/J K^{-1} mol^{-1}	$\Delta G^{\ddagger}$ (298.15 K)/ kJ mol^{-1}
		2,4,6-TMNB			
$Z\text{-D} \rightleftharpoons 2\text{M}$	1D-TD	223–243	85.8 ± 3.5	59 ± 14	68.35 ± 0.08
$Z\text{-D} \rightleftharpoons 2\text{M}$	2D-EXSY	253–263			
$E\text{-D} \rightleftharpoons 2\text{M} \overset{\text{fast}}{\rightleftharpoons} Z\text{-D}$	1D-TD	273–283	104.7 ± 2.4	55 ± 8	88.51 ± 0.03
$E\text{-D} \rightleftharpoons 2\text{M}$	2D-EXSY	313–333			
		2,4,6-TBNB + NB			
$E\text{-D} \rightleftharpoons 2\text{M} \overset{\text{fast}}{\rightleftharpoons} Z\text{-D}^a$	1D-TD	283–303	121.6 ± 1.3	115 ± 4	87.27 ± 0.02

[a] Mixed dimers.

Table 5. Rate data for E-(2,4,6-TMNB)$_2$ ⟶ 2(2,4,6-TMNB) exchange.

NMR method	T/K	$10^3\text{K}/T$	k/s^{-1}	$\ln(k/T)$
1D-TD	273	3.663	3.59×10^{-5}	−15.84
	283	3.534	2.08×10^{-4}	−14.12
2D-EXSY	313	3.195	1.22×10^{-2}	−10.16
	323	3.096	5.18×10^{-2}	−8.73
	333	3.003	2.12×10^{-1}	−7.37

Therefore, $k_{-1} = k_1[E\text{-D}]_e/[\text{M}]^2_e$
Let $p = [E\text{-D}]_e/[\text{M}]_e^2 = k_{-1}/k$. Substituting into equation (5), gives equation (7).

$$\frac{d[\text{M}]}{dt} = 2k_1[E\text{-D}] - 2k_1p[\text{M}]^2 - 4K_e[\text{M}]\frac{d[\text{M}]}{dt} \quad (7)$$

Substitution for c in equation (7) and rearranging gives equations (8) and (9).

$$\frac{d[\text{M}]}{dt} = k_1X - 4K_e[\text{M}]\frac{d[M]}{dt}$$

where $$X = c - [\text{M}] - [\text{M}]^2(2p + 2K_e)$$

$$\frac{d[\text{M}]}{X} + 4K_e[\text{M}]\frac{d[\text{M}]}{X} = k_1dt \quad (8)$$

$$\int_{[\text{M}]_0}^{[\text{M}]_t}\frac{d[M]}{X} + 4K_e\int_{[\text{M}]_0}^{[\text{M}]_t}\frac{[\text{M}]d[\text{M}]}{X} = \int_0^t k_1dt \quad (9)$$

In equation (9) the monomer concentrations $[\text{M}]_0$ and $[\text{M}]_t$ refer to times $t = 0$ and $t = t$.

Integration of equation (9) (see Appendix) gives the rate law, equation (10), where the parameters a, b, v, w, x, y, and z

$$A\ln\left\{\frac{x[\text{M}]_t + a}{y[\text{M}]_t + b}\right\} + B\ln\left\{\frac{v[\text{M}]_t^2 - [\text{M}]_t + c}{w}\right\} = -zk_1t \quad (10)$$

are functions of concentrations $[\text{M}]_0$ and $[\text{M}]_e$ (see Appendix). The E-dimer ⟶ monomer rate constants k_1 can, therefore, be deduced from the slope of the LHS of equation (10) *versus* time. Values were calculated for temperatures 273 and 283 K, (Table 5).

2D-EXSY *NMR studies*, 313–333 K. In this temperature range the concentration of Z-(2,4,6-TMNB)$_2$ was negligibly low, whereas the E-dimer and monomer species were present in equilibrium concentrations and their exchange rates could, therefore, be suitably monitored by the 2D-EXSY method.[26]

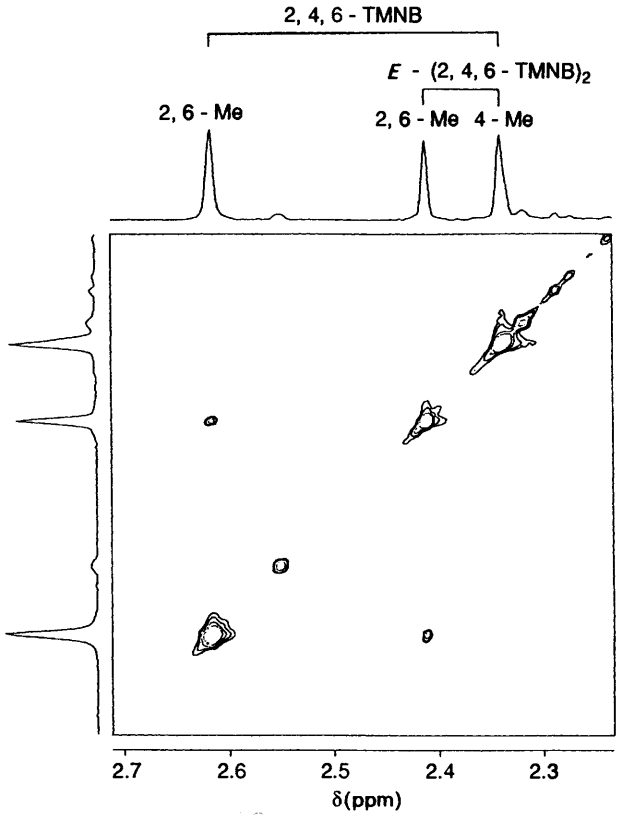

Figure 2. Proton NMR 2D-EXSY spectrum of 2,4,6-TMNB in $CDCl_3$ at 323 K showing the E-2,4,6-(TMNB)$_2$ ⟶ 2 (2,4,6-TMNB) exchange. Mixing time τ_m = 1.5 s.

The 2D spectrum measured at 323 K (Figure 2) exemplifies the method. The highest frequency signal (δ *ca.* 2.62) is due to the 2,6-methyl groups of the monomer 2,4,6-TMNB and the signal at δ 2.42 due to the corresponding methyls of E-(2,4,6-TMNB)$_2$. Some weak impurity signals were also present but they were not involved in any exchange process. Well defined cross peaks are observed, indicating the E-dimer–monomer exchange. The third signal, which is somewhat broader than the others, is due to the 4-methyl protons of both monomeric and E-dimeric 2,4,6-TMNB (see Table 1). Rate constants were measured from relative intensities of the 2,6-methyl signals using the D2DNMR program.[25] The resulting values (Table 5) were then combined with the values derived from the time-dependent studies in the form of an Eyring plot (Figure 3). Both sources of rate data gave good consistency indicating the validities of both kinetic methods. Activation energy parameters derived from this graph are contained in Table 4.

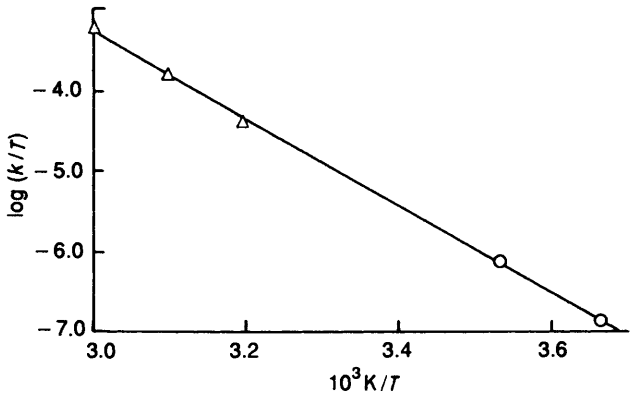

Figure 3. Eyring plot of rate data for the *E*-(2,4,6-TMNB)$_2$ ⟶ 2 (2,4,6-TMNB) dissociation using time-dependent 1D NMR data (○) and 2D-EXSY NMR data (△).

Table 6. Proton chemical shifts of 2,4,6-TMNB + NB in $CDCl_3$[a] at 303 K.

δ[b]	2,6-Me	4-Me
2.63	2,4,6-TMNB	
2.42	*E*-(2,4,6-TMNB)$_2$	
2.34		2,4,6-TMNB
2.33	*E*-(2,4,6-TMNB/NB)	*E*-(2,4,6-TMNB)$_2$
2.32		*E*-(2,4,6-TMNB/NB)
2.24	*Z*-(2,4,6-TMNB/NB)	
2.23		*Z*-(2,4,6-TMNB/NB)

[a] 0.1 mol dm^{-3} solution. [b] Relative to Me_4Si.

Table 7. Proton chemical shifts of 2,4,6-TBNB + NB in $CDCl_3$[a] at 283 K.

Band No.[b]	δ[c]	2,6-t-butyl	4-t-butyl
1	1.444	*E*-(2,4,6-TBNB/NB)	
3	1.346		*E*-(2,4,6-TBNB/NB)
5	1.329		*Z*-(2,4,6-TBNB/NB)
6	1.323		2,4,6-TBNB
7	1.247	Z-(2,4,6-TBNB/NB)	
8	1.231	2,4,6-TBNB	

[a] 0.1 mol dm^{-3} solution. [b] See Figure 4. Bands 2 and 4 are due to 2,4,6-tri-t-butylnitrobenzene. [c] Relative to Me_4Si (int.).

2,4,6-*Trimethylnitrosobenzene* (2,4,6-TMNB) + *Nitrosobenzene* (NB).—An earlier NMR study[16] on the mixed systems 2,6-DMNB + NB and 2,6-DMNB + 3,5-DMNB identified mixed azodioxy dimers. It was, therefore, of interest to investigate whether 2,4,6-TMNB would also form mixed dimers in the presence of NB. An equimolar mixture of 2,4,6-TMNB and NB in $CDCl_3$ was, therefore, examined by ^1H NMR in the temperature range 273–303 K, and the methyl absorption region analysed. Seven signals were identified (Table 6) although at certain temperatures this number was reduced owing to chemical shift overlaps. Signals due to 2,4,6-TMNB and *E*-(2,4,6-TMNB)$_2$ were assigned immediately by comparison with previous data (Table 1). The remaining signals were clearly associated with both *Z* and *E* mixed dimers (2,4,6-TMNB/NB). Unambiguous assignments of the 2,6- and 4-methyl signals of these mixed dimers were not possible, but the assignment given in Table 6 is most favoured by analogy with previous shift data.[16] The spectra, however, show clearly that both mixed dimeric species are present in solution in comparable amounts. No kinetic studies were performed on account of the spectral complexity.

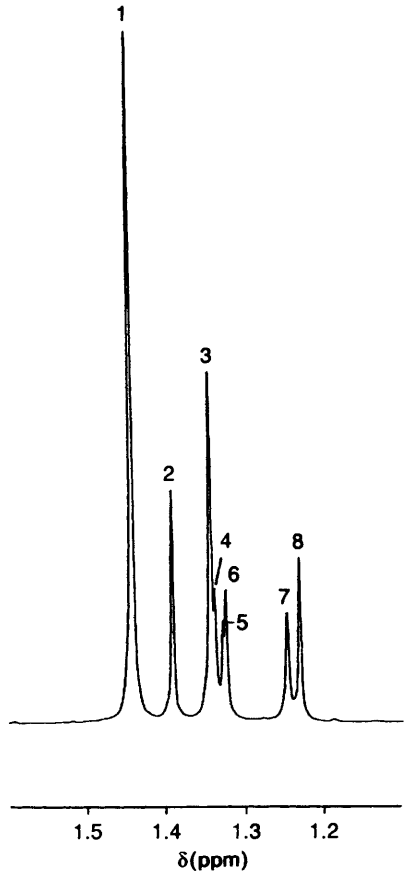

Figure 4. 250 MHz ^1H NMR spectrum (methyl region) of 2,4,6-TBNB + NB in $CDCl_3$ at 283 K showing the formation of both mixed azodioxy dimers. See Table 7 for signal numbering and assignments.

2,4,6-*Tri-t-butylnitrosobenzene* (2,4,6-TBNB).—This compound is widely used as a spin-trapping agent,[22] its efficacy in this respect depending, among other things, on its stable monomeric nature both in the solid and solution states.[21] It was, therefore, judged important to investigate whether there was any appreciable dimerisation in the presence of other nitrosobenzene species as this would be pertinent to its radical scavenging abilities.

Proton NMR spectra of a commercial sample of 2,4,6-TBNB were measured in the temperature range 223–303 K. Its two t-butyl signals and one aromatic signal did not change significantly throughout this temperature range confirming that the monomeric state was maintained at all times. Additional weak signals in the spectra were attributed to a small amount of 2,4,6-tri-t-butylnitrobenzene impurity (*ca.* 5%).

2,4,6-*Tri-t-butylnitrosobenzene* (2,4,6-TBNB) + *Nitrosobenzene* (NB).—An equimolar mixture (0.1 mol dm^{-3} with respect to both monomers) in $CDCl_3$ was studied in the temperature range 283–303 K. The aromatic and methyl regions of the ^1H NMR spectra clearly indicated the presence of dimers and since neither monomer forms significant quantities of self association dimers in this temperature range, then the presence of mixed 2,4,6-TBNB/NB dimers was indicated. Figure 4 depicts the methyl region of the ^1H NMR spectrum at 283 K. Eight signals were resolved of which two are due to the 2,4,6-tri-t-butylnitrobenzene impurity (Table 7). The assignments are

fairly certain, those for the 2,6-t-butyl groups of the monomer and mixed dimers being unambiguous. The populations of the two mixed dimers are very different, the preferred species being attributed to *E*-(2,4,6-TBNB/NB) since both 2,6-DMNB[16] and 2,4,6-TMNB dimerise more favourably into the *E* forms. Admittedly, the favoured dimer of nitrosobenzene is *Z*-$(NB)_2$, but steric effects of the methyl and t-butyl substituents are thought to be overriding factors in determining the nature of thermodynamically favoured mixed dimeric species.

In the temperature range 283–303 K the equilibrium of *Z*-(2,4,6-TBNB/NB) with the two monomers is fast in contrast with the slow exchange occurring with *E*-(2,4,6-TBNB/NB). The kinetic system is given by Scheme 5.

$$E\text{-(2,4,6-TBNB/NB)} \underset{k_{-1}}{\overset{k_1}{\rightleftharpoons}} \text{2,4,6-TBNB} + \text{NB} \overset{\text{fast}}{\rightleftharpoons} Z\text{-(2,4,6-TBNB/NB)}$$

Scheme 5.

The kinetics of this system are analogous to that of 2,4,6-TMNB in the temperature range 273–283 K (see above). Time-dependent NMR studies were, therefore, performed, as previously, using in this case the 2,6-t-butyl signals of 2,4,6-TBNB and *E*-(2,4,6-TBNB/NB) as probes of the exchange rates. The results for three temperatures are given in Table 8, and activation energy data in Table 4. It would have been preferable to have extended this temperature range somewhat. However, the system was not amenable to this, since raising the temperature caused the population of *E*-(2,4,6-TBNB/NB) to approach its equilibrium population too rapidly (< 1 min), and lowering the solution temperature led to an unsuitably low concentration of the 2,4,6-TBNB monomer.

An attempt was made to measure the rate of exchange of *Z*-(2,4,6-TBNB/NB) with 2,4,6-TBNB using 2D-EXSY spectra, but the very small chemical shift differences of the t-butyl signals in these species (Figure 4) resulted in unreliable and inconsistent rate data.

Discussion

The trends in activation parameters for the dimer–monomer dissociations of 2,4,6-TMNB and 2,4,6-TBNB (Table 4) are more usefully discussed in the context of earlier studies on 2,6-DMNB and NB (Table 9). As a result of the positive entropy terms, $\Delta S^{\ddagger}$, typical of dissociation equilibria, the $\Delta G^{\ddagger}$ values decrease significantly with increasing temperature. At 298 K values range from 88.5 kJ mol^{-1} for *E*-$(2,4,6\text{-TMNB})_2$ to 64.9 kJ mol^{-1} for *Z*-$(2,6\text{-DMNB})_2$. This variation is primarily a consequence of differing ground-state energies of these species. The *E*-azodioxy dimers are clearly stabilised by the presence of alkyl groups on the 2 and 6 ring positions (*cf.* 2,6-DMNB or 2,4,6-TBNB with NB, Table 9). This also leads to appreciable differences in $\Delta G^{\ddagger}$ values for the dissociation of *E*- and *Z*-dimers of the same monomer. This difference is > 20 kJ mol^{-1} for 2,4,6-TMNB and 2,6-DMNB, but only *ca.* 4 kJ mol^{-1} for NB itself. Dissociation energies of mixed dimers are expected to be close to the mean values for the pure dimers. Thus, the $\Delta G^{\ddagger}$ value for the dissociation of *E*-(2,6-DMNB/NB) is 79.44 kJ mol^{-1} which is very near to 79.0 kJ mol^{-1}, the mean of the *E*-$(2,6\text{-DMNB})_2$ and *E*-$(NB)_2$ dissociation values. Given the validity of that observation, if any *E*-$(2,4,6\text{-TBNB})_2$ was to be formed it would subsequently dissociate with a high activation energy ($\Delta G^{\ddagger}$ would be *ca.* 104 kJ mol^{-1}).

Table 8. Rate data for *E*-(2,4,6-TBNB/NB) ⟶ 2,4,6-TBNB + NB exchange.

T/K	$10^3 K/T$	k/s^{-1}	$\ln(k/T)$
283	3.534	2.2×10^{-4}	−14.07
293	3.413	1.29×10^{-3}	−12.33
303	3.300	7.13×10^{-3}	−10.66

Conclusions

In summary, it has been shown that 2,4,6-trimethylnitrosobenzene forms *Z*- and *E*-self-association dimers in $CDCl_3$ with the *E*-dimer appreciably more favoured. In the presence of nitrosobenzene, mixed azodioxy species are also formed. The spin trapping agent 2,4,6-tri-t-butylnitrosobenzene shows no tendency towards self-association but will dimerise readily in the presence of nitrosobenzene to form *Z*- and *E*-mixed species with the latter more highly favoured. A judicious combination of 1D time-dependent and 2D-EXSY ^1H NMR techniques has enabled the kinetics of these systems to be accurately measured over a wide temperature range.

Acknowledgements

We wish to thank Dr. R. B. Moodie of this Department for his helpful comments on the kinetic analyses.

References

1 B. G. Gowenlock and W. Lüttke, *Q. Rev. Chem. Soc.*, 1958, **12**, 321, and references therein.
2 P. A. Smith, 'The Chemistry of Open Chain Nitrogen Compounds,' Benjamin, New York, 1966, vol. 2, ch. 13.
3 J. H. Boyer, in 'The Chemistry of Nitro and Nitroso Groups,' ed. H. Feuer, Part 1, Wiley, New York, 1968, p. 215.
4 G. Sandler and H. Kara, in 'Organic Preparations of Functional Groups,' ed. A. Blomquist, Academic Press, New York, 1971, vol. 12, part 2.

Table 9. Activation parameters for the dissociation of aromatic nitrosobenzene dimers.

Compound	Process	$\Delta G^{\ddagger}$(298 K)/ kJ mol^{-1}	$\Delta H^{\ddagger}$/kJ mol^{-1}	$\Delta S^{\ddagger}$/J K^{-1} mol^{-1}	Ref.
2,4,6-TMNB	*E* D ⟶ M	88.51 ± 0.03	104.7 ± 2.4	55 ± 8	This work
	Z D ⟶ M	68.35 ± 0.08	85.8 ± 3.5	59 ± 14	This work
2,6-DMNB	*E* D ⟶ M	87.9 ± 0.1	118 ± 1	100 ± 3	16
	Z D ⟶ M	64.9 ± 0.4	97 ± 2	108 ± 10	16
2,6-DMNB + NB	*E* D[a] ⟶ M	79.44 ± 0.01	112 ± 6	110 ± 19	16
	Z D[a] ⟶ M	71.96 ± 0.03	97 ± 10	85 ± 32	16
2,4,6-TBNB + NB	*E* D[a] ⟶ M	87.27 ± 0.02	121.6 ± 1.3	115 ± 4	This work
NB	*E* D ⟶ M	70.0 ± 0.3	94 ± 4	82 ± 16	15
	Z D ⟶ M	65.8 ± 0.1	89 ± 1	76 ± 3	15

[a] Mixed, unsymmetrical dimer.

5 D. L. H. Williams, 'Nitrosation,' Cambridge University Press, Cambridge, 1987.
6 S. Darwin and D. C. Hodgkin, *Nature*, 1950, **166**, 827.
7 C. P. Fenimore, *J. Am. Chem. Soc.*, 1950, **72**, 3226.
8 D. A. Dieterich, I. C. Paul, and D. Y. Curtin, *J. Am. Chem. Soc.*, 1974, **90**, 6372.
9 K. Nakamoto and R. E. Rundle, *J. Am. Chem. Soc.*, 1956, **78**, 1113.
10 A. Gruger, N. Le Calve, and J. Fillaux, *Spectrochim. Acta, Part A*, 1975, **31**, 595.
11 M. Azoulay, B. Stymne, and G. Wettermark, *Tetrahedron*, 1976, **32**, 2961.
12 M. Azoulay and G. Wettermark, *Tetrahedron*, 1978, **34**, 2591.
13 M. Azoulay, R. Lippman, and G. Wettermark, *J. Chem. Soc., Perkin Trans. 2*, 1981, 256.
14 M. Azoulay and E. Fischer, *J. Chem. Soc., Perkin Trans. 2*, 1982, 637.
15 K. G. Orrell, V. Šik, and D. Stephenson, *Magn. Reson. Chem.*, 1987, **25**, 1007.
16 K. G. Orrell, D. Stephenson, and T. Rault, *Magn. Reson. Chem.*, 1989, **27**, 368.
17 D. L. Hammick, W. A. M. Edwards, W. S. Illingworth, and F. R. Snell, *J. Chem. Soc.*, 1933, 671.
18 L. R. C. Barclay, D. L. Carson, J. A. Gray, M. Grossman, P. G. Khazanie, J. R. Milton, and C. E. Scott, *Can. J. Chem.*, 1978, **56**, 2665.
19 V. A. Batyuk, T. I. Shabatina, Yu. N. Morozov, S. V. Ryapisov, and G. B. Sergeev, *Vestn. Mosk. Univ. Ser. 2 Khim.*, 1988, **29**, 270.
20 V. von Keussler and W. Lüttke, *Z. Electrochem.*, 1959, **63**, 614.
21 R. Okazaki, T. Hosogai, E. Iwadare, M. Hashimoto, and N. Inamoto, *Bull. Chem. Soc. Jpn.*, 1969, **42**, 3611.
22 M. J. Perkins, in 'Advances in Physical Organic Chemistry,' eds. V. Gold and D. Bethell, Academic Press, London, 1980, vol. 17.
23 S. Terabe and R. Konaka, *J. Chem. Soc., Perkin Trans. 2*, 1973, 369.
24 G. H. Coleman, C. M. McCloskey, and F. A. Stuart, *Org. Synth.*, 1945, **25**, 80.
25 E. W. Abel, T. P. J. Coston, K. G. Orrell, V. Šik, and D. Stephenson, *J. Magn. Reson.*, 1986, **70**, 34.
26 R. Willem, *Prog. Nucl. Magn. Reson. Spectrosc.*, 1987, **8**, 1.
27 S. Forsén and R. A. Hoffman, *J. Chem. Phys.*, 1963, **39**, 2892.
28 J. Jeener, B. H. Meier, P. Bachmann, and R. R. Ernst, *J. Chem. Phys.*, 1979, **71**, 4546.
29 S. Macura and R. R. Ernst, *Mol. Phys.*, 1980, **41**, 95.
30 C. L. Perrin and R. K. Gipe, *J. Am. Chem. Soc.*, 1984, **106**, 4036.
31 T. Beringhelli, G. D'Alfonso, H. Molinari, G. E. Hawkes, and K. D. Sales, *J. Magn. Reson.*, 1988, **80**, 45.
32 R. C. Weast, 'Handbook of Chemistry and Physics,' 62nd edn., Chemical Rubber Company, Cleveland, Ohio (1981–82), pp. A-37, 38.

Appendix

For the kinetic Scheme 4

$$E\text{-D} \underset{k_{-1}}{\overset{k_1}{\rightleftharpoons}} 2\text{M} \overset{\text{fast}}{\rightleftharpoons} Z\text{-D}$$

where Z-D and M are in rapid equilibrium, the approach of E-D and M to equilibrium concentrations follows the integrated rate law, equation (9)

$$\int_{[\text{M}]_o}^{[\text{M}]_t} \frac{\text{d}[\text{M}]}{X} + 4K_e \int_{[\text{M}]_o}^{[\text{M}]_t} \frac{[\text{M}]\text{d}[\text{M}]}{X} = \int_o^t k_1 \text{d}t \qquad (9)$$

where $X = c - [\text{M}] - [\text{M}]^2(2p + 2K_e)$.

Tables of standard integrals[32] give equations (9*a* and *b*)

$$\int \frac{\text{d}x}{X} = \frac{1}{\sqrt{-q}} \ln\left(-\frac{2cx - b + \sqrt{-q}}{2cx + b + \sqrt{-q}}\right) \qquad (9a)$$

$$\int \frac{x\text{d}x}{X} = \frac{1}{2c} \ln X - \frac{b}{2c} \int \frac{\text{d}x}{X} \qquad (9b)$$

where $X = a + bx + cx^2$ and $q = 4ac - b^2$.

Using these results in equation (9), and evaluating between the limits, leads, after some rearrangment, to the following equation (9*c*).

$$\frac{p}{p + K_e} \ln \frac{\{([\text{M}]_e - [\text{M}]_t)\}\{[\text{M}]_o(c - [\text{M}]_e) + c[M]_e\}}{\{([\text{M}]_e - [\text{M}]_o)\}\{[\text{M}]_t(c - [\text{M}]_e) + c[\text{M}]_e\}} +$$

$$\frac{\sqrt{-q}K_e}{p + K_e} \ln\left\{\frac{-2[\text{M}]_t^2(p + K_e) - [\text{M}]_t + c}{-2[\text{M}]_o^2(p + K_e) - [\text{M}]_o + c}\right\} = -\sqrt{-q}k_1 t \qquad (9c)$$

This can be expressed as equation (10).

$$A_t \ln\left(\frac{x[\text{M}]_t + a}{y[\text{M}]_t + b}\right) + B \ln\left(\frac{v[\text{M}]_t^2 - [\text{M}]_t + c}{w}\right) = -zk_1 t \qquad (10)$$

where $A = p/(p + K_e)$

$B = K_e z/(p + K_e)$

$a = [\text{M}]_e\{[\text{M}]_o(c - [\text{M}]_e) + c[\text{M}]_e\}$

$b = ([\text{M}]_e - [\text{M}]_o)c[\text{M}]_e$

c = total solution concentration expressed as monomer moieties, $v = -2(p + K_e)$, $w = v[\text{M}]_o^2 - [\text{M}]_o + c$, $x = -\{[\text{M}]_o(c - [\text{M}]_e) + c[\text{M}]_e\}$, $y = (c - [\text{M}]_e)([\text{M}]_e - [\text{M}]_o)$, $z = \sqrt{-q} = (2c - [\text{M}]_e)/[\text{M}]_e$.

First-order E-D ⟶ M rate constants, k_1, may, therefore, be evaluated from the slope of the graph of the LHS of equation (10) *versus* time.

Paper 9/03957K
Received 18*th September* 1989
Accepted 2*nd April* 1990